One-dimensional Phase-Change Nanowires for Information Storage Application

Xuhui Sun, Bin Yu

Ames Center for Advanced Aerospace Materials and Devices
NASA Ames Research Center, Moffett Field, CA 94035
xsun@arc.nasa.gov (XHS) byu@arc.nasa.gov (BY)

ABSTRACT

The electrically operated phase-change random access memory (PRAM) features faster write/read, improved endurance, and much simpler fabrication as compared with the traditional transistor-based nonvolatile semiconductor memories. Low-dimensional phase-change materials in nanoscale dimensions offer advantages over their bulk or thin-film counterpart in several aspects such as reduced programmable volume and reduced thermal energies in phase transition. These features contribute to low power operation, excellent scalability, and fast write/erase time. In this paper we reported a general bottom-up synthesis approach and systematic material analysis study of one-dimensional chalcogenide-based phase-change materials including germanium telluride (GeTe), indium selenide (In_2Se_3), and germanium antimony telluride ($Ge_2Sb_2Te_5$) nanowires that are targeted for nonvolatile resistive switching data storage. The phase-change nanowires have been synthesized via thermal evaporation method under vapor-liquid-solid (VLS) mechanism. The morphology, composition, and crystal structure of the synthesized nanowires were investigated by scanning electron microscopy, energy dispersive X-ray spectroscopy, and high-resolution transmission electron microscopy. The as-synthesized nanowires are structurally uniform with single crystalline structures. The 1-D phase-change chalcogenide nanowires exhibit significantly reduced melting points, low activation energy and excellent morphology, making them promising nanomaterials for data storage devices with very low energy consumption and excellent scalability.

Keywords: phase-change materials, nanowires, PRAM

1 INTRODUCTION

Information storage employing alternative, non-charge-based state variables (such as material structural phase or electron spin) represents a major trend in future nanoelectronics. Phase-change materials (PCMs) are among the most promising media for nonvolatile, re-writable, and highly endurable data storage.[1-8] Phase-change memories rely on binary or multiple reflective/resistive states of the programmable element to represent the logic levels for data storage. The optical reflectivity or electrical resistance in the material is reversibly switched due to thermally induced transition between two stable material phases: the orderly single crystalline or polycrystalline phase (c-phase) and the less orderly amorphous phase (α-phase). In particular, resistive switching PRAM features faster write/read, improved endurance, and much simpler fabrication as compared with the transistor-based nonvolatile memories. Because the data is stored in the form of material phases, PRAM offers soft-error- or radiation-free operation.

A major issue limiting the extensive use of thin-film-based PRAM is the enormous programming current to generate the thermal energy needed for phase change. This is particularly a concern in the crystal to amorphous (c-to-α) phase transition when high current is required for melting. The Joule heating effect may cause power dissipation issues and inter-cell thermal interference, preventing possibilities for future scaling. The phase change behavior of chalcogenide materials in the nanoscale may overcome these limitations [9-10] and therefore warrant a detailed investigation.

2 EXPERIMENTAL DETAILS

Our experiment was carried out in a vacuum furnace system. High-purity GeTe, In_2Se_3 and the mixture of GeTe and Sb_2Te_3 powders were placed in the middle of the high-temperature zone for GeTe, In_2Se_3 and $Ge_2Sb_2Te_5$ nanowires growth, respectively. Gold nanoparticles (20 nm) were dispersed as catalyst on thermal SiO_2 coated Si (100) substrate for nanowire growth. The substrate was placed downstream in the reactor tube at low temperature zone. The reactor tube was evacuated to a base pressure of 10^{-2} torr prior to the experiment. Ar as the carrier gas, was introduced at a flow rate of 25-100 sccm (standard cubic centimetres per minute) and at a pressure of 200 torr – 1atm. The temperatures for nanowires growth are: 400~450°C for GeTe and $Ge_2Sb_2Te_5$, 650~700°C for In_2Se_3 nanowires. The morphology and structure of the synthesized products were characterized by scanning electron microscopy (Hitachi S-4000 FEG) and transmission electron microscopy (TEM Philips CM20, operated at 200 kV) equipped with energy dispersive X-ray spectroscopy (EDS) for chemical composition analysis. The nanowires were dispersed onto the SiO_x-film-coated TEM grids and were subjected to a real-time melting point measurement experiment under the TEM.

3 RESUTLS AND DISCUSSION

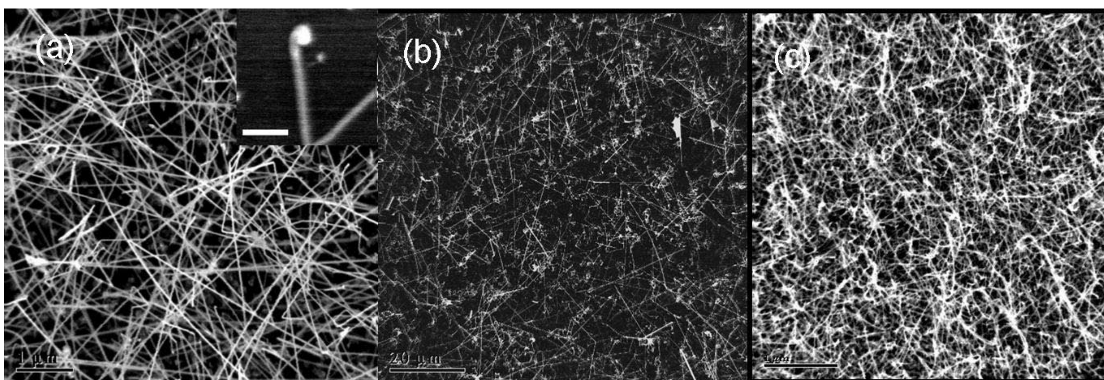

Figure 1: SEM image of the as-synthesized (a) GeTe nanowires, (b) In_2Se_3 nanowires and (c) $Ge_2Sb_2Te_5$ nanowires on SiO_2-coated Si (100) substrate using 20 nm Au nanoparticles as growth catalyst. Scale bars are: 1μm in (a), 20 μm in (b) and 1μm in (c). Inset of (a) is a close-up view of a catalyst bead at the tip of the single GeTe nanowire. Scale bar (inset) is 200 nm.

Figure 1 shows SEM images of the as-synthesized GeTe, In_2Se_3 and $Ge_2Sb_2Te_5$ nanowires on the surface of SiO_2 substrate, showing high-yield nanowire growth. The nanowires have a diameter in the range of 40~80 nm and are up to tens of micrometers in length. Au catalyst beads are visible at the tips of the nanowires as seen in the inset of Fig 1(a), implying that the nanowires were possibly grown under the VLS mechanism.

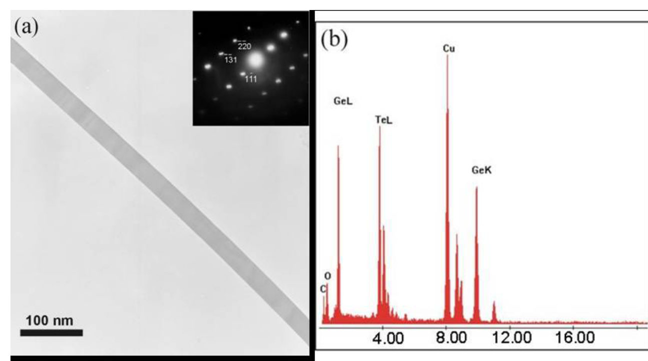

Figure 2. (a) Low-magnification TEM image of an individual GeTe nanowire with a diameter of about 40 nm. The inset shows the SAED pattern of an fcc cubic lattice structure. (b) EDS spectrum of the same GeTe nanowire as shown in (a).

Further structural characterization of the GeTe nanowires was performed with TEM. Figure 2(a) shows a low-magnification TEM image of a single GeTe nanowire with uniform diameter of about 40 nm along its entire length. Selected Area Electron Diffraction (SAED) pattern taken from the nanowire (shown in the inset) reveals that the nanowire is a single crystal with cubic lattice structure. The EDS analysis of an individual nanowire with locally focused beam spot confirms that the nanowire is composed of only germanium and tellurium with an atomic ratio close to 1:1. The trace O peak is from the oxide outer layer. The high-resolution TEM (HR-TEM) image analysis further indicates that the as-prepared GeTe nanowires are high-quality single crystals. Figure 3(a) and 3(b) show that the GeTe nanowire is structurally uniform and contains no noticeable defects such as dislocations and stacking faults. A layer of 1~3 nm amorphous oxides shell, covering the GeTe nanowire surface which exhibits an atomically sharp interface, was formed probably either during the growth due to oxygen leakage or afterwards when the nanowires were exposed to the ambient environment. It is known that the surface of GeTe is oxidized spontaneously in the presence of atmospheric air to form $GeO_2 \cdot TeO_2$.[13-14] The lattice spacing of ~3.5 Å in Figure 3(a) and ~2.1 Å in Figure 3(b) corresponds to the d-spacing of the (111) and (220) crystal planes, respectively, of GeTe with a cubic lattice structure. HR-TEM imaging results and SAED pattern suggest that the GeTe nanowire is single crystal of the cubic structure with lattice constant a of ~6.01 Å, which is consistent with the JCPDS PDF 03-065-0415 (cubic structure, Fm3m, a=6.02 Å). The GeTe nanowires have a preferential growth direction in the <110> crystalline orientation.

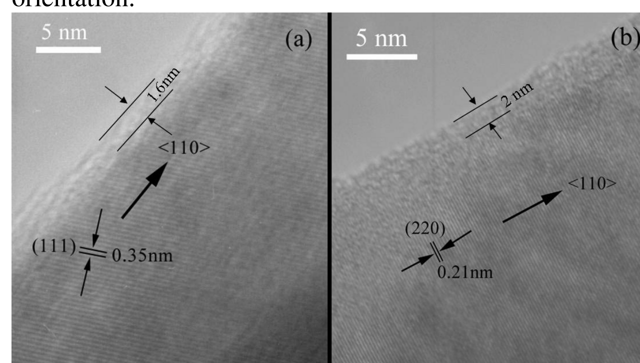

Figure 3. High-resolution TEM images of the crystal structure of GeTe nanowires. (a) From one sample the individual GeTe nanowire shows (111) planes with an interplane spacing of ~0.35 nm. (b) From another sample the GeTe nanowire shows (220) planes with an interplane spacing of ~0.21 nm. Both nanowire samples show an elongation along the preferential <110> crystalline

NSTI-Nanotech 2007, www.nsti.org, ISBN 1420061828 Vol. 1, 2007

orientation. A thin (1~3nm) amorphous oxide layer is observed on the surface of GeTe nanowire in both samples.

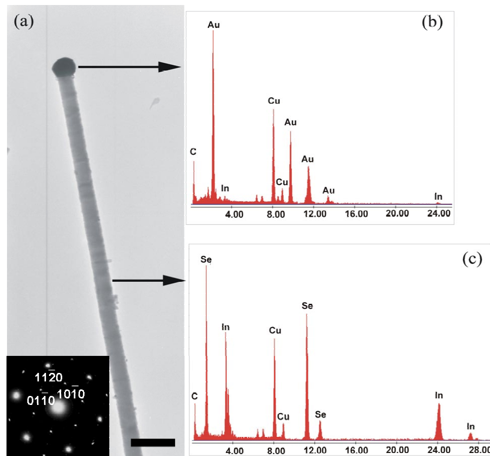

Figure 4. (a) TEM image of In_2Se_3 NW grown on SiO_2 substrate using 20 nm gold nanoparticles as catalyst. A metal bead is observed at the tip of the nanowire. Scale bar is 200 nm. SAED pattern taken on the same NW is shown in inset. (b) EDS spectrum with locally focused e-beam spot on the bead part (arrow indicated). 5.0 at.% In: 95.0 at.% Au was detected. (c) EDS spectrum with locally focused e-beam spot on the nanowire part (arrow indicated).

A representative TEM image (Fig. 4a) of an individual In_2Se_3 NW shows that the nanowire has smooth surface and uniform thickness along the growth direction. Local EDS analyses (Fig. 4b) shows that the particle, the dark-colored ball on the tip of the nanowire (Fig. 4a), is composed primarily of gold. Indium content is below 5 at. % and selenium content is below the detection level. The local point EDS analysis on the nanowire (Fig. 4c), shows that In and Se are present in an approximately 2:3 atomic ratio. The Cu and C signals shown in the spectra are from carbon-coated copper TEM grid. The selected area electron diffraction (SAED) pattern taken on the same nanowire shows regular spot patterns (Fig. 4a inset), which confirms the single crystalline nature of the nanowires. The diffraction spots in the SAED pattern can be indexed to β-phase In_2Se_3 hexagonal structure, and the growth direction of the nanowire is along [110] direction determined together with HR-TEM images analysis as follows.

A representative TEM image (Fig. 5a) shows that the $Ge_2Sb_2Te_5$ (GST) nanowire has a smooth surface with metal particle clearly noticeable on the tip (bottom inset, Fig. 5a), indicating that the growth process followed the vapor-liquid-solid (VLS) mechanism. Local EDS analyses in which the TEM electron beam is focused on a targeted sample areas as small as 9 nm in diameter, shows that the particle, the dark-colored ball on the tip of the nanowire, is composed primarily of gold. Local EDX analysis of the individual nanowire discloses that Ge, Sb and Te are present approximately in an atomic ratio of 2:2:5 (Fig. 5c). The Si, O and Cu signals in EDX spectrum are from SiO_x-film-coated copper TEM grid. Both SAED pattern (top inset, Fig. 5a) and HR-TEM image (Fig. 5b) confirm the single crystalline nature of the GST NWs. The SAED pattern shows regular spot patterns, which further confirms the perfect single crystalline nature of the NWs. The diffraction spots in the SAED pattern can be indexed to cubic fcc structure with lattice constant a of ~6.0 Å, and the growth direction of the NW is along the <111> direction. The HR-TEM image (Fig. 5b) shows the planes with a lattice spacing of ~3.0 Å that corresponds to d-spacing of the (200) plane of GST fcc structure. The angle, $\alpha = 54.7°$, in the image fits the one between the (200) plane and (111) plane, which indicates that the nanowire comprises a preferential growth direction in the <111> direction.

For phase change materials, the melting point (T_m) is an important physical property relevant to the performance of data storage devices. Lower T_m represents that the c-to-α phase transition, corresponding to the memory reset activity, can be executed with a lower thermal energy. In our investigation, the T_m of GeTe nanowires was measured via an *in-situ* heating experiment in a TEM chamber under real-time morphology monitoring. In the setup, the sample

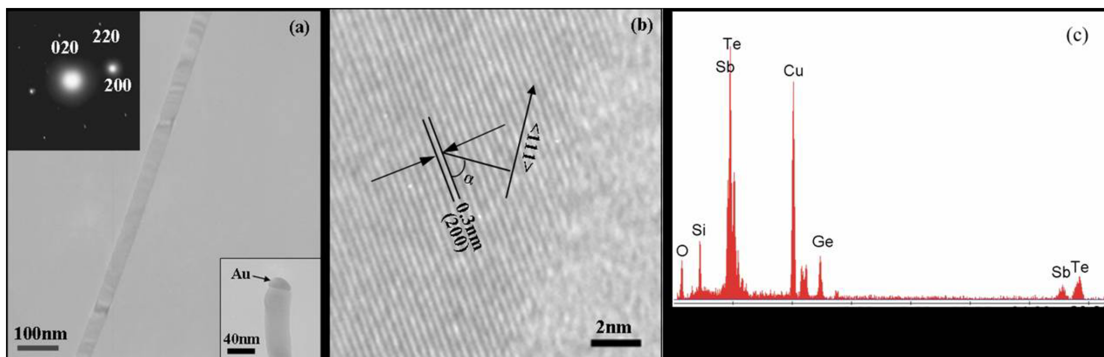

Figure 5. (a) TEM image of an individual GST NW. Top left inset: SAED pattern of an fcc cubic structure. Bottom right inset: Au particle at the NW tip. (b) HR-TEM image of the (200) planes of fcc GST. (c) EDX spectrum of individual GST NW shown in (a).

stage was resistively heated at a rate of 10°C/min. The melting temperature of the nanowire is identified as the point at which the electron diffraction pattern disappears and the nanowire starts to be evaporated. The melting and evaporation process of the GeTe nanowires was monitored in real time by TEM and recorded by a video camera in the bright-field mode.

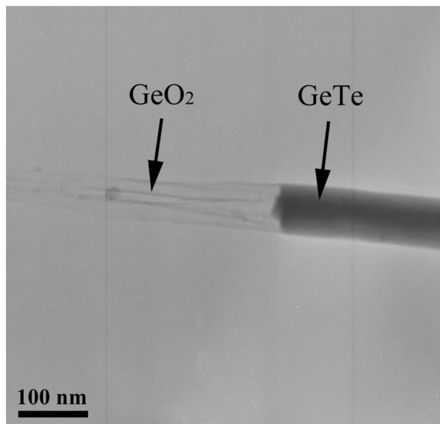

Figure 6. Measurement of the melting point of a single germanium telluride nanowire under real-time TEM morphology monitoring. The GeTe nanowire is heated up to 400°C. The nanowire is molten and its mass is gradually lost through evaporation. The remaining oxide nanotube can be clearly seen from the image.

We observed a significant drop of T_m for GeTe nanowire from that for bulk GeTe. GeTe nanowires started melting at 390°C, which is 46% less than the bulk melting point of GeTe (725°C). Upon reaching the T_m (390°C), the contrast of GeTe nanowire was abruptly turn to dark and the electron diffraction pattern disappeared as the material changed from solid crystalline phase to liquid phase. The molten nanowire further vaporized out from the two open ends of the nanowire and a nanotube structure left behind. A TEM image was taken during the evaporation process, as shown in Figure 6. The very thin wall of the remaining tube, confirmed from EDS analysis, is the GeO_2 oxide outerlayer of GeTe nanowire. Because bulk GeO_2 (T_m: 1115°C) has much higher melting point than that of bulk GeTe and TeO_2 (T_m: 733°C), it turns out that only GeO_2 shell was left behind when the temperature was increased up to the T_m of GeTe nanowire. The native GeO_2 outerlayer provides an excellent nature protection in the device performance in which no extra outerlayer is needed in the device fabrication to prevent oxidation and evaporation. The real-time recorded melting and evaporation process by video camera is shown in the supporting materials. The melting point reduction in GeTe nanowires does not show size dependence in the diameter range of 40 nm-80 nm, which is not consistent with the previous reports for metal particles [15] and semiconductor nanocrystals [16] that found a dependence on particle radius. It is probably due to small diameter range studied in this experiment that does not make distinguished change of melting point. The smaller diameter may result in possible lower melting point. The exact mechanism of phase changes and the dependency of the phase change properties as a function of nanowire size in nanoscale need to be further explored.

4 CONCLUSIONS

In summary, we have presented a bottom-up approach to synthesize a one-dimensional chalcogenide phase-change material: GeTe, In_2Se_3 and $Ge_2Sb_2Te_5$ nanowires. Single crystalline phase change nanowires with non-lithographically defined diameter down to 40 nm have been produced via metal-catalyzed VLS growth. The GeTe nanowire has a measured melting point as low as 390°C, significantly reduced from that of bulk GeTe, and therefore exhibits great potential for future data storage application with low thermal energy required for phase switching operation.

REFERENCES

[1] Ovshinsky, S. R. *Phys. Rev. Lett.* 21, 1450, **1968**.
[2] Adler, D.; Shur, M. S.; Silver, M.; Ovshinsky, S. R. *J. Appl Phys*., 51, 3289, **1980**
[3] Chen, M.; Rubin, K.; Barton, R. *Appl. Phys. Lett*., 49, 502, **1986**.
[4] Coombs, J.; Jongenelis, A.; van Es-Spiekman, W.; Jacobs, B. *J. Appl. Phys.*, 78, 4906, **1995**.
[5] Volkert, C. A.; Wuttig, M. *J. Appl. Phys*., 86, 1808, **1999.**
[6] Yamada, N.; Matsunaga, T. *J. Appl. Phys*. 88, 7020, **2000**.
[7] Lai, S.; Lowrey, T. in *IEDM Tech Dig*., 803, **2001.**
[8] Pirovano, A.; Lacaita, A. L.; Benvenuti, A.; Pellizzer, S.; Bez, R. *IEEE Trans Elec. Dev*., 51, 452, **2004.**
[9] Lankhorst, M. H. R.; Ketelaars, B. W. S. M. M.; Wolters, R. A. M. *Nat Mater*, *4*, 347-352, **2005.**
[10] Yu, D.; Wu, J. Q.; Gu, Q. A.; Park, H. K. *J. Am. Chem. Soc*., *128*, 8148-8149, **2006**.
[11] Meister, S.; Peng, H. L.; McIlwrath, K.; Jarausch, K.; Zhang, X. F.; Cui, Y. *Nano Letters*, *6*, 1514-1517, **2006**.
[12] Yamada, N.; Ohno, E.; Nishiuchi, K.; Akahira, N.; Takao, M. *J Appl Phys*, *69*, 2849, **1991.**
[13] Gogishvili, O. S.; Degaltsev,.A. N.; Kononov, G. G.; Lavrinenko, I. P.; Lalykin, S. P. *Inorg. Mater.*, *24*, 944, **1988.**
[14] Sheveleva, T. F.; Plaksina, Y. B.; Markholiya, T. P. *Inorg. Mater. 12*, 791, **1976**.
[15] Buffat, Pho; Borel, J.P., *Phys. Rev.*, 13, 2287, **1976**.
[16] Goldstein, A.N.; Echer, C.M.; Alivisatos, A.P., *Science*, 256, 1425, **1992**.